Computer Fraud and Security
ISSN (online): 1873-7056

Heavy Fog Image Enhancement Algorithm Based on Tophat Weighted Bilateral Filtering

Zihong Chen, Xiaoling Zhang, Liangyan Wang
School of Modern Health and Regimen Industry, Anhui Sanlian University, Hefei, China

Abstract:
A Retinex algorithm based on Tophat weighted bilateral filtering is proposed to enhance the distortion of images in highly heavy foggy weather, which makes it difficult to recognize objects. Firstly, The Tophat operator is used to correct the bilateral filter, keeping the edge effects of the brightness component. Then, an adaptive Gamma transformation is applied to expand the details of the saturation and brightness of the dark tones, and the reflection component is obtained from the illumination component through the Retinex algorithm to further enhance the detail information of the heavy image. Finally, the enhanced image is obtained by converting the HSV color space model into the RGB color space. The enhancement effect was evaluated from both subjective and objective aspects. The subjective evaluation results showed that the gray-scale range of the image was more reasonable, and objects in the image could be recognized more clearly. In terms of objective evaluation, when compared with the Retinex algorithm with color restoration (MSRCR), guided filter Retinex algorithm (GFR), improved dark prior algorithm, and Frankle-McCann Retinex algorithm (FMR), the proposed method greatly improved in terms of information entropy, standard deviation, and average gradient. The defogging effect was significantly improved.

Keywords: tophat operator, HSV model, retinex algorithm, bilateral filter

INTRODUCTION

The visibility level of haze refers to the ability of people to distinguish target objects in the sky background under normal weather conditions. When the visibility is less than 0.3 kilometers, it is considered heavy fog, and when it is less than 0.1 kilometers, it is considered extremely dense fog [1]. Currently, image defogging algorithms can be divided into two major types: those based on image restoration and those based on image enhancement [2]. The former includes methods based on deep learning, prior information, and light polarization properties, which aims to analyze the process of image degradation to improve contrast and highlight image details [3]. However, these methods have their limitations in dealing with thick fog or extremely dense fog. The latter type includes methods such as histogram equalization-based algorithms, wavelet transform-based algorithms, homomorphic filtering, and Retinex algorithm [4-6]. Among these, the Retinex algorithm is the most commonly used one, as it focuses on enhancing the image details, but it has the drawback of ignoring the assumption of uniform lighting, which can lead to image blurring and distortion of the edge contours [7-10].

To address these limitations, this paper proposes a Retinex algorithm based on Tophat-weighted bilateral filtering for enhancing images in extremely foggy weather. The Tophat operator is used to correct the bilateral filter and applied as a filtering function to the brightness component to maintain its edge effect [11]. An adaptive Gamma transformation is applied to extend the saturation and brightness details of the dark tones, while the reflection component is obtained.

PROCESS CONSTRUCTION

Conversion between RGB and HSV Models

In the conversion from RGB to HSV, the maximum intensity of the RGB components is denoted as $I_{max} = \max(R, G, B)$, while the minimum intensity is denoted as $I_{\min} = \min(R, G, B)$. The intensity range is calculated based on I_{max} and I_{min} using equation $I_{diff} = I_{max} - I_{min}$ [12]. Therefore, the calculation of H, S, and V is shown in Equations (1), (2), and (3).

$$H=\begin{cases}0 & \text{if } I_{\max}=I_{\min}\\ \left(60^{\circ}\times\dfrac{G-B}{I_{\text{diff}}}+0^{\circ}\right)\bmod 360^{\circ} & \text{if } I_{\max}=R\\ \left(60^{\circ}\times\dfrac{B-R}{I_{\text{diff}}}+120^{\circ}\right) & \text{if } I_{\max}=G\\ \left(60^{\circ}\times\dfrac{R-G}{I_{\text{diff}}}+240^{\circ}\right) & \text{if } I_{\max}=B\end{cases} \tag{1}$$

$$S=\begin{cases}0 & \text{if } I_{\max}=0\\ \dfrac{I_{\text{diff}}}{I_{\max}} & \text{else}\end{cases} \tag{2}$$

$$V=I_{max} \tag{3}$$

Moreover, the equation used for converting from the HSV color space to the RGB color space is shown in Equation (4).

$$(r,g,b)=\begin{cases}(v,t,p), & \text{if } h_1=0\\ (q,v,p), & \text{if } h_1=1\\ (p,v,t), & \text{if } h_1=2\\ (p,q,v), & \text{if } h_1=3\\ (t,p,v), & \text{if } h_1=4\\ (v,p,q), & \text{if } h_i=5\end{cases} \tag{4}$$

In the above equation, $p=v(1-s)$, $q=v(1-fs)$, $t=v[1-(1-f)s]$, among them, $f=\dfrac{h}{60}-h_i$, $h_i=\left\lfloor\dfrac{h}{60}\right\rfloor(\bmod 6)$; mod is a modular operation. $\lfloor\ \rfloor$ is the bottom symbol [13].

Enhance Algorithm Process Construction

The Retinex algorithm based on Tophat-weighted bilateral filtering is used to enhance foggy images, and the enhancement process is shown in Figure 1, with the specific steps as follows:

(1) The input image is converted from the RGB color space to the HSV color model image, which is separated into three channel components: hue (H), saturation (S), and value (V).

(2) The Tophat operator is used to correct the bilateral filter by convolving with the brightness component to extract the brightness component.

(3) An adaptive Gamma correction function is used to adjust the illumination and saturation components separately, obtaining the corrected illumination and saturation components.

(4) Based on the corrected illumination component obtained in step (3), the Retinex algorithm is used to obtain the reflection component.

(5) After the HSV model channels are merged, the hue component, the corrected saturation component, and the reflection component are converted back to the RGB color space.

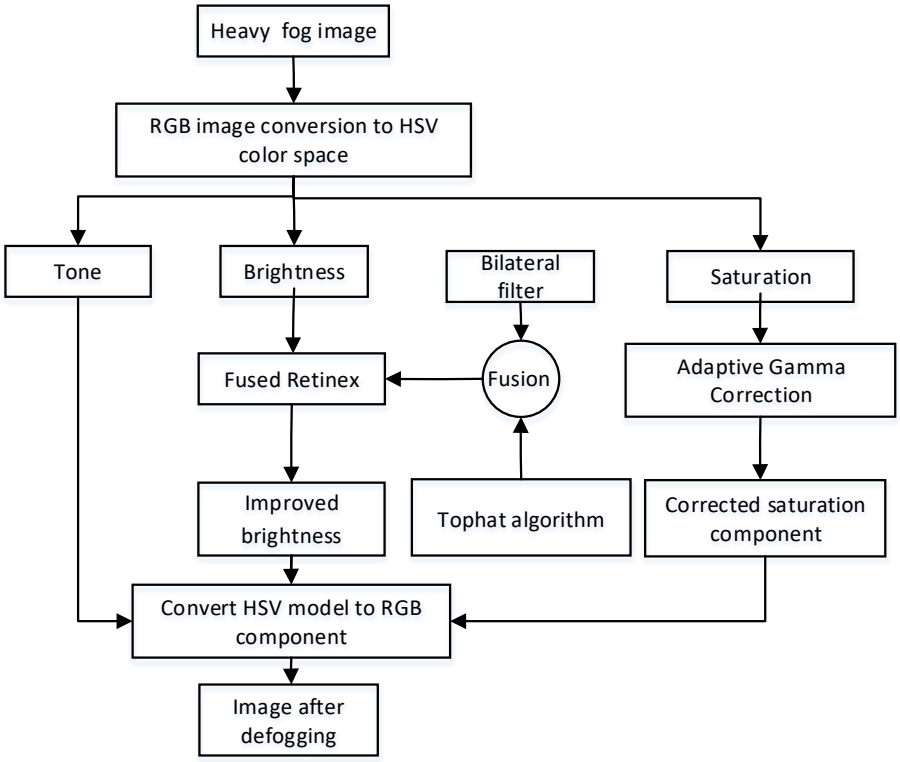

Figure 1. Algorithm flow chart

RETINEX ALGORITHM BASED ON TOPHAT WEIGHTED BILATERAL FILTER

Image Enhancement Based on Retinex Algorithm

In the Retinex model, the image F can be regarded as the product of the reflection part R and the illumination part L, as shown in Equation (5):

$$F = L \cdot R \tag{5}$$

After taking the logarithm of Equation (5), the following Equation (6) is obtained:

$$\log R = \log F - \log L \tag{6}$$

In Equation (6), the illumination part L is obtained by convolving the perceived image F with the filter function H, which is equivalent to the following Equation (7):

$$\log R = \log F - \log(H \otimes F) \tag{7}$$

The central idea of the Retinex image enhancement algorithm is to use the filter function H to re-calculate the illumination part L and reflection part R of the image, and then perform the Retinex inverse transformation to obtain a haze-free image [14]. In this paper, the Retinex algorithm based on Tophat weighted bilateral filtering is used to extract the luminance component, and the adaptive Gamma function is used to adjust the illumination and saturation components separately. Finally, the illumination, chrominance, and saturation components are merged to obtain a haze-free image.

Tophat Weighted Guided Bilateral Filtering

Bilateral filtering is used to adjust the value of w, so that the weight corresponding to the part of the image with obvious texture is higher, leading to larger image information entropy. Usually, when using Wiener filtering or Gaussian filtering for de-noising, there is obvious edge blur, but bilateral filtering is a non-linear filter that includes two components: spatial domain weight and signal domain weight. Bilateral filtering cannot filter out high-frequency noise in hazy images cleanly, but it can filter low-frequency information well. Therefore, the

protection effect of bilateral filtering on high-frequency details in an image is not obvious [15]. For heavy fog images, it is difficult to obtain appropriate edge weight factors by only calculating the information entropy. The bilateral filtering function in the input image F, with N(x) as the center neighborhood, is defined by the following Equation (8):

$$J(x)=\frac{\sum_{y\in ¥(x)} F(y)\omega\left(x,y,\sigma_s\right)\omega\left(F(x),F(y),\sigma_r\right)}{\sum_{y\in N(x)} \omega\left(x,y,\sigma_s\right)\omega\left(F(x),F(y),\sigma_r\right)} \tag{8}$$

In the equation above, the pixel x is calculated by weighted mean calculation. Compared with Gaussian filter, bilateral filter has an additional mask, which takes into account not only the spatial distance relationship between pixels but also the degree of similarity between pixel values. Therefore, bilateral filter has anisotropy and can preserve the texture and details of the image. The Gaussian kernel ω is defined as shown in Equation (9):

$$\omega(s,t,\sigma)=\exp\left(-\frac{\| s-t \|^2}{2\sigma^2}\right) \tag{9}$$

In the definition of the Gaussian kernel shown in the equation above, σ_s and σ_r are the standard deviations in the spatial domain and pixel value respectively. Tophat transformation is actually the difference between the original image and the result image of "opening operation". It is a morphological transformation method in image processing and can extract local bright areas in relatively dark background images [16]. The extraction method is shown in the Equation (10) below:

$$\mathrm{g}(x,y)=\begin{cases} I(x,y)-\mathrm{open}(I(x,y)), I(x,y)\geq \mathrm{open}(I(x,y)) \\ 0 \qquad \text{others} \end{cases} \tag{10}$$

The result of Tophat transformation is to magnify the local low brightness area [17]. Subtracting the result of opening operation from the original image can highlight the brighter area than the surrounding area of the original image. Therefore, the detail information of bright areas will be enhanced. To further preserve the high-frequency information of the image[18], this paper proposes the Tophat algorithm with weighted guided bilateral filter as the Retinex filter function, as shown in Equations (11), (12), and (13) below.

$$w=(1-\theta)\omega\left(x,y,\sigma_s\right)+\theta\omega\left(F(x),F(y),\sigma_r\right) \tag{11}$$

$$\theta=\frac{\mathrm{Entropy}(F)}{2\,\mathrm{Entropy}(N(x))} \tag{12}$$

$$J(x)=\frac{\sum_{y\in ¥(x)} F(y)w(x,y)}{\sum_{y\in N(x)} w(x,y)} \tag{13}$$

Where w represents the weight of the signal domain, Entropy(F) and Entropy(N(x)) are the information entropy of the original image and the de-hazed image neighborhood. In the low-frequency part of the image, the information is relatively small, and the corresponding θ value is larger. At this time, the weight coefficient w tends to be the frequency domain weight; in the high-frequency part of the image, the corresponding signal quantity is larger, and θ is smaller, so the weight coefficient w tends to be the spatial domain weight [19]. The filtering effects of different algorithms are shown in the Figure 2 below.

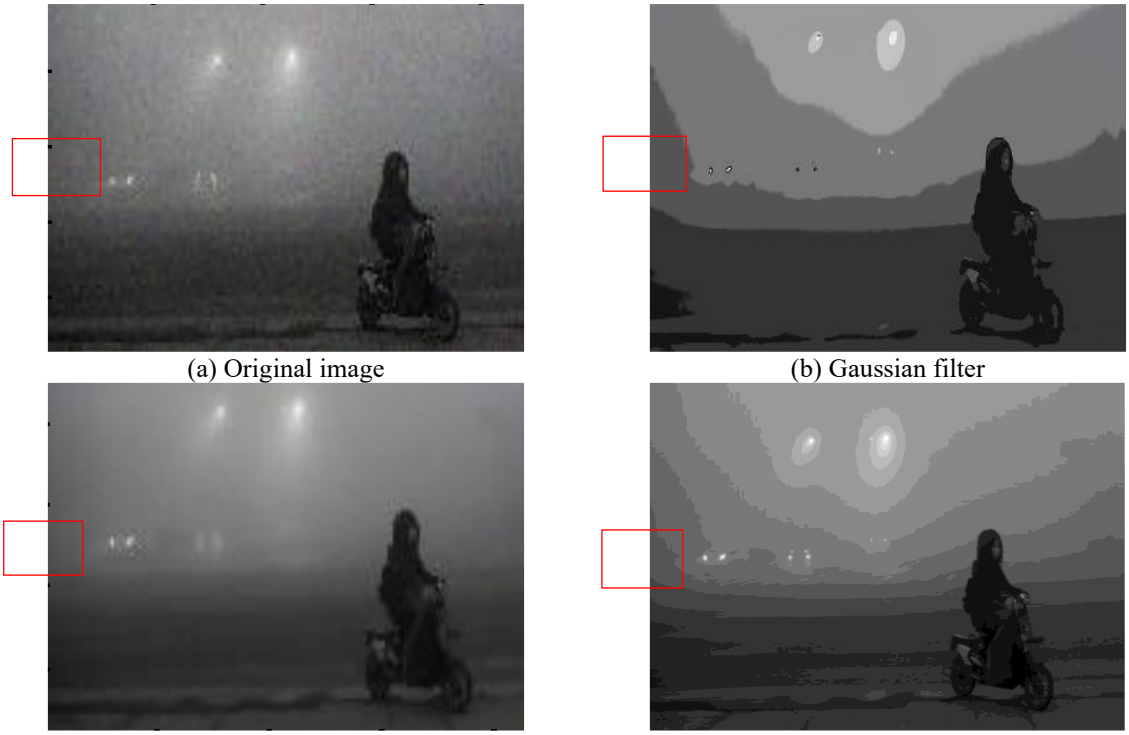

(a) Original image (b) Gaussian filter

(c) bilateral (BF) filtering (d) Proposed algorithm

Figure 2. Comparison of filtering effects of different algorithms

From Figure 2, it can be seen that under similar smoothing effects, the proposed algorithm can better preserve the edge information of the image.

Extracting the Luminance Component

After bilateral filtering with Tophat weighting, The algorithm in this paper extracts the illumination component using Equation (14):

$$F(x,y) = G\left(I, r_i, w_n, s\right) \tag{14}$$

In the above equation: $F(x,y)$ represents the estimated illumination component based on the guided image I; G represents the Tophat-weighted bilateral filtering operation applied to the guided image I; w_n represents the edge weight factor; s represents the down-sampling factor, and the edge weight factor is given by Equation (15).

$$w_n = \frac{1}{N}\sum_{n=1}^{N}\frac{T(m)+\alpha}{T(n)+\alpha} \tag{15}$$

Where wn is the edge weighting factor, N is the number of pixels in the bilateral filter, T(m) is the mean value of the image after Tophat transformation with pixel m as the window center, T(n) is the mean value of the bilateral filtered image with pixel n as the window center, and α is a constant with a value of 1×10^{-4}. The enhanced brightness component is shown in Figure 3 after luminance enhancement.

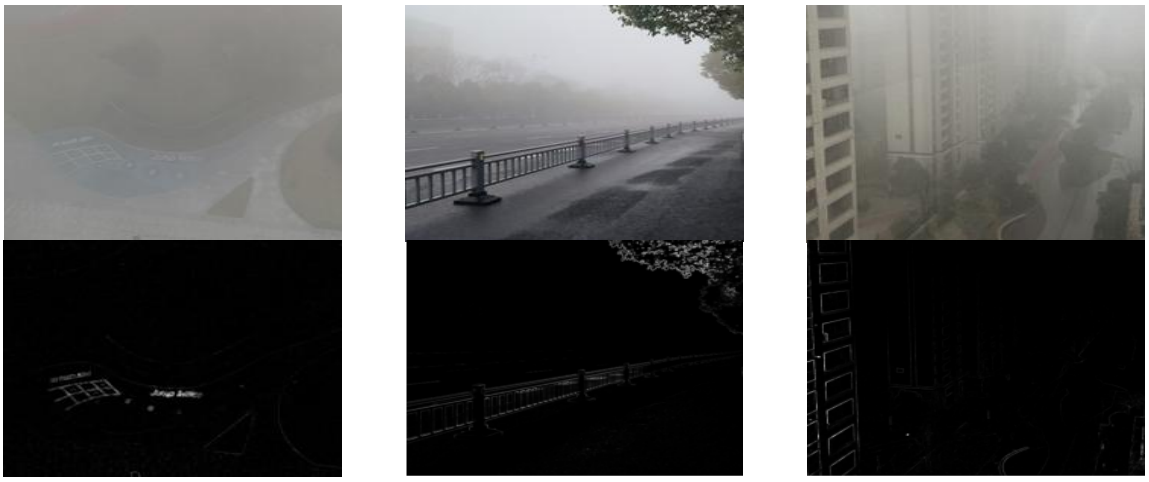

(a)Brightness of the first image (b) Brightness of the second image (c) Brightness of the third image

Figure 3. The enhancement of the brightness component in heavy images.

From Figure 3, it can be seen that Tophat weighted bilateral filtering can better preserve high-frequency components and extract image edge details. For regions with high image brightness, the edge weight factor wn larger and the corresponding θ is smaller, which can better preserve the image detail information of the high-brightness area. For regions with low image brightness, the edge weight factor wn is smaller and the corresponding θ is larger, which results in better smoothing effect for low-brightness regions.

Brightness and Saturation Correction

An adaptive Gamma correction function is utilized to enhance the illumination and saturation components, resulting in a more uniform brightness and preserved saturation details [20,21]. The transformation equation is shown as Equation (16):

$$Z(x,y) = 255\left(\frac{F(x,y)}{255}\right)^{\left(1-\frac{1}{\gamma}\right)} \tag{14}$$

In the above equation, Z(x,y) represents the corrected illumination component, and γ represents the adaptive gamma correction coefficient, which is critical to the brightness of the image. The image enhancement effect for different values of γ is shown in Figure 4.

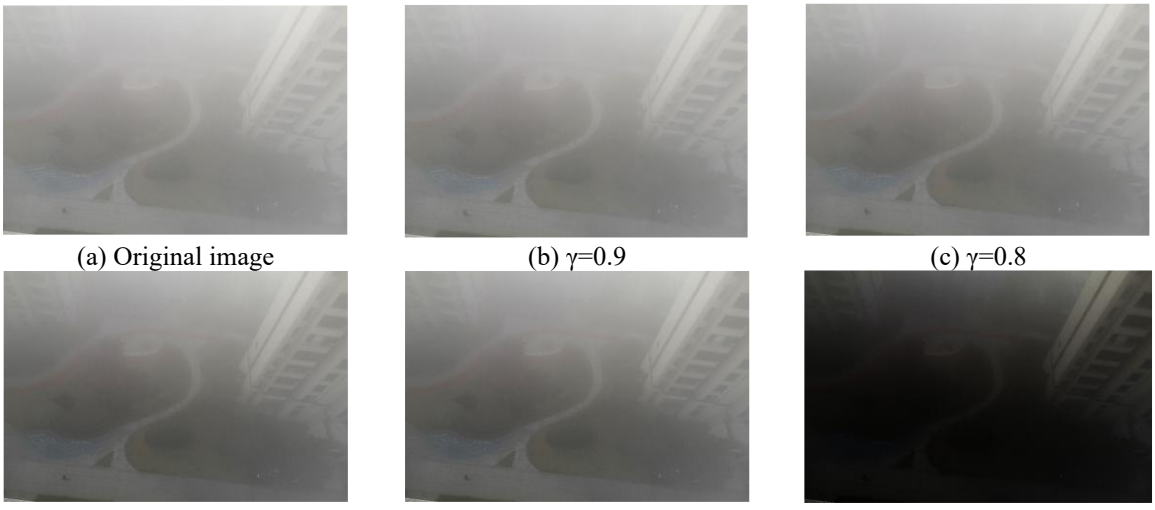

(a) Original image (b) γ=0.9 (c) γ=0.8

(d) γ=0.6 (e) γ=0.4 (f) γ=0.2

Figure 4. Comparison of correction effects under different values of γ

When γ is less than 0.4, the image appears to have over-saturation. When γ=0.6, the brightness of the dark areas of the image is enhanced without excessive enhancement of the bright areas. When γ=0.8, the overall brightness

enhancement of the image is not significant. Therefore, the illumination component correction coefficient used in this paper is 0.6.

After enhancing the brightness of the image and correcting the saturation in the HSV color space, the image can be converted from the HSV color space to the RGB color space to complete the enhancement of the foggy image.

EXPERIMENTAL ANALYSIS

To verify the defogging effect of the proposed Tophat-weighted bilateral filtering, close range and distant view images were used for testing under heavy foggy weather conditions, where the visibility level was less than 100 meters at the time of image collection. The Multi-scale Retinex with color restoration algorithm (MSRCR) [22], Guided Filter Retinex algorithm (GFR) [23], improved image enhancement algorithm based on the dark prior principle [24], Frankle-McCann's Retinex filtering algorithm (FMR) [25], and the proposed Tophat-weighted bilateral filtering defogging algorithm were used to enhance the close range and distant view images, and the resulting images were evaluated subjectively and objectively.

Subjective Evaluation

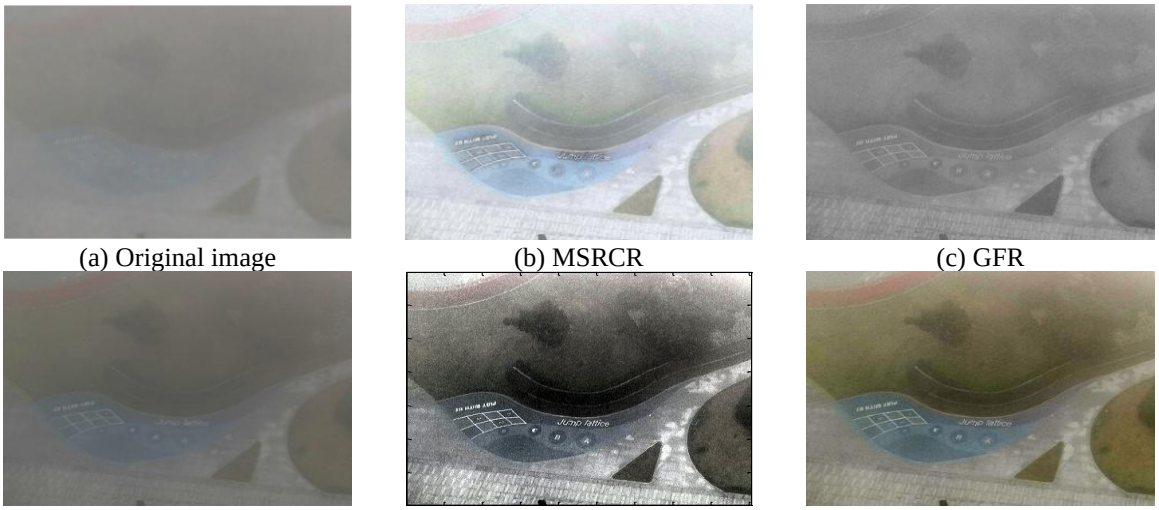

(a) Original image (b) MSRCR (c) GFR

(d) Improved dark prior principle (e) FMR (f) Proposed algorithm

Figure 5. The subjective comparison on the close range image

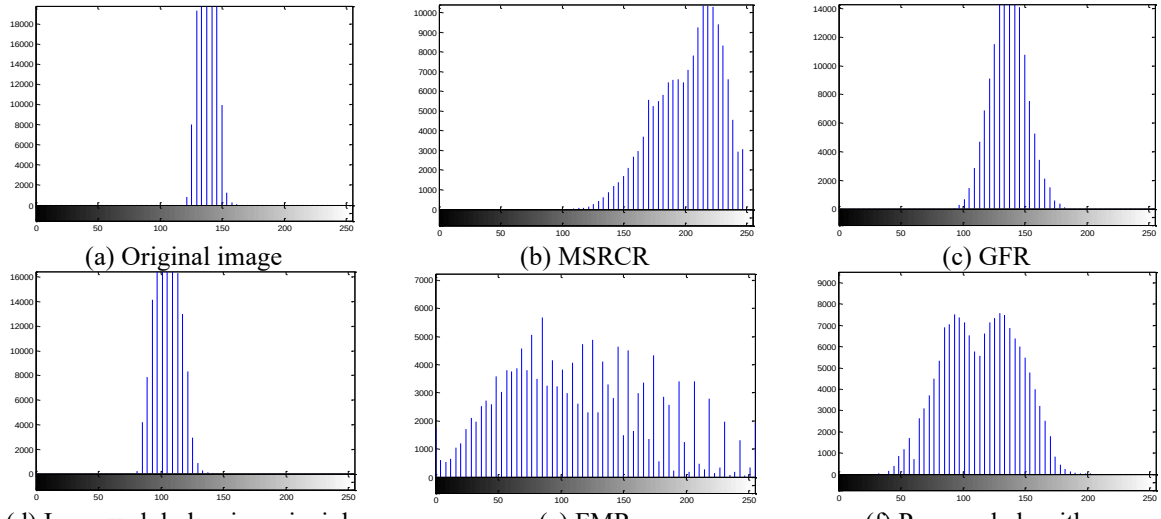

(a) Original image (b) MSRCR (c) GFR

(d) Improved dark prior principle (e) FMR (f) Proposed algorithm

Figure 6. The grayscale histogram comparison on the close range image

To better compare the contrast effects of the enhanced images under heavy foggy weather conditions, the grayscale histogram was used as an auxiliary comparison tool. If the image has high contrast, then its grayscale distribution is uniform and extensive. Figure 5 shows the visual comparison results of the various algorithms on

the close range object, and Figure 6 shows the histograms of the enhanced images, which were used to assist in judging the enhancement effects of the various algorithms.

Figure 5(b) can identify the ground text, but there is a halo phenomenon in the upper right corner lawn area. Figure 5(c) can enhances the overall contrast of the image, but the grayscale histogram distribution is relatively narrow and the color is dull. Figure 5(d) has a narrow grayscale distribution. Figure 5(e) is a pyramid comparison model. The grayscale level distribution of the image enhanced by this method is too large, resulting in color distortion and excessive brightness; Figure 5(f) can clearly identify ground letters in the enhanced distant image. The histogram distribution is relatively uniform and broad, and the rubber runway and its surrounding area in the upper left corner are also displayed clearly.

Figure 7 and Figure 8 show the comparison of the enhancement effects and histogram distribution of the distant view images.

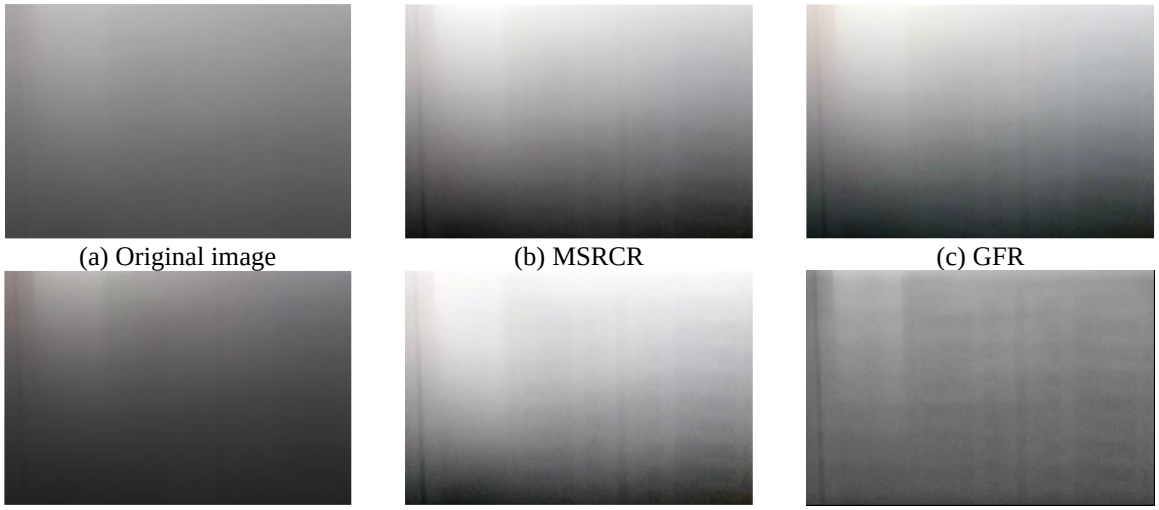

(a) Original image (b) MSRCR (c) GFR

(d) Improved dark prior principle (e) FMR (f) Proposed algorithm

Figure 7. Subjective comparison for distant view images

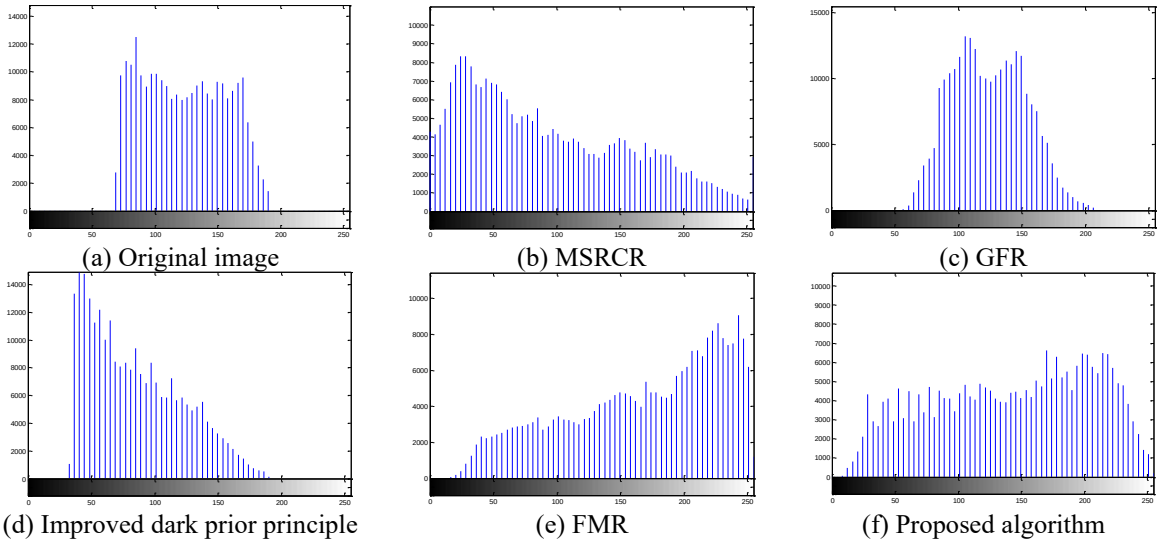

(a) Original image (b) MSRCR (c) GFR

(d) Improved dark prior principle (e) FMR (f) Proposed algorithm

Figure 8. Histogram comparison for distant view images

In Figure 5, Figure 5(a) shows the original image of the close range in heavy fog, in which the text on the ground in the small area is very blurry and cannot be recognized. Figure 5(b) shows the image enhanced by the MSRCR algorithm, which can identify the ground text, but there is a halo phenomenon in the upper right corner lawn area. Figure 5(c) shows the image enhanced by the Retinex algorithm based on guided filtering, which enhances the overall contrast of the image, but the grayscale histogram distribution is relatively narrow and the color is dull. Figure 5(d) shows the enhanced image by the classic dark channel prior algorithm, which has a narrow grayscale distribution. Figure 5(e) shows the enhancement algorithm based on Frankle-McCann Retinex,

which is a pyramid comparison model. Iterations are carried out layer by layer from the top to the bottom of the pyramid with increasing resolution. The grayscale level distribution of the image enhanced by this method is too large, resulting in color distortion and excessive brightness; Figure 5(f) shows the algorithm proposed in this study, which can clearly identify ground letters in the enhanced distant image. In Figure 6, the histogram distribution is relatively uniform and broad, and the rubber runway and its surrounding area in the upper left corner are also displayed clearly.

Figure 6(a) shows the original image captured in distant view image, in the Figure 5(b), the objects remain indistinguishable. In the Figure 6(c), a building can be vaguely seen in the lower-right corner but still unclear. The Figure 6(d), also failed to identify any objects. The Figure 6(e) can identify the presence of buildings in the image; however, the overall brightness is high and the histogram analysis indicates high grayscale values. In Figure 6(f), the outlines of buildings can be clearly distinguished and the floors can be vaguely perceived, with a more uniform grayscale histogram.

Figure 7(a) shows the original image captured in distant view image, where all objects are blurred and indistinguishable. Figure 7(b) shows the image enhanced by the MSRCR algorithm, but the objects remain indistinguishable. Figure 7(c) demonstrates the results obtained by the Retinex algorithm based on guided filtering, where a building can be vaguely seen in the lower-right corner but still unclear. Improved dark prior principle, as presented in Figure 7(d), also failed to identify any objects. The Frankle-McCann Retinex approach shown in Figure 7(e) manages to identify the presence of buildings in the image, however, the overall brightness is high and the histogram analysis indicates high grayscale values. Figure 7(f) presents the results of the proposed algorithm, where the outlines of buildings can be clearly distinguished and the floors can be vaguely perceived, with a more uniform grayscale histogram.

Objective Evaluation

Objective evaluation uses Peak Signal-to-Noise Ratio (PSNR), Information Entropy, Standard Deviation, Mean Gradient, Mean, and Variance as evaluation standards for image enhancement algorithms. The MSRCR algorithm, GFR algorithm, improved dark prior principle, FMR algorithm, and the algorithm proposed were separately used to enhance close-range and distant view images in the verification process. The verification results can be seen in Tables 1 and 2.

Table 1. Objective evaluation of close-range image enhancement effects

Algorithm category	PSNR	Information Dentropy	Standard Deviation	Mean Gradient	Mean	Variance
Original image.	——	8.6685	7.2183	0.9533	137.4728	52.1049
MSRCR	16.6227	10.1445	33.0809	5.1134	110.448	1094.35
GFR	28.5150	5.81307	13.6902	4.3320	136.7072	187.423
Improved dark prior principle	17.5391	8.65745	10.7779	1.9417	103.8814	116.1631
FMR	11.3615	13.8578	28.3019	6.3355	202.4731	800.9985
Proposed algorithm	16.0068	10.2858	34.6992	5.6892	108.3848	1204.034

Table 2. Objective evaluation of distant view image enhancement effects

Algorithm category	PSNR	Information Dentropy	Standard Deviation	Mean Gradient	Mean	Variance
Original image.	——	11.5962	42.5153	0.8289	152.3403	1807.5513
MSRCR	20.58821	11.6734	58.7242	1.7001	138.8492	3487.4305
GFR	21.8396	7.06973	36.2046	2.8690	144.1331	1310.7748
Improved dark prior principle	14.5980	11.0889	48.8373	1.2803	106.0208	2385.0895
FMR	18.1537	12.6293	48.0395	2.0509	180.2507	2307.7973
Proposed algorithm	20.0138	11.7172	59.5170	1.8693	134.6491	3542.2768

Table 1 shows that for the close-rang images, the information entropy of the image is increased by 18.6%, which is higher than the dark prior principle, BFR, and MSRCR algorithms. The gradient of the image is significantly higher than the original image and is higher than the MSRCR, BFR, and dark prior principle. The gradient is

improved by 10.8% compared to MSRCR algorithm. The standard deviation of the images in this study is increased by 380.7% compared to the original image, which is the greatest among all these algorithms. The standard deviation is 4.9% higher than the classic MSRCR algorithm, and the variance is 10.0% higher than the MSRCR algorithm. However, the average grayscale value of the image is low, indicating an overall low grayscale value.

Table 2 shows that for the distant view images, the information entropy of the image is increased by 1.2% compared to the original image, which is higher than the algorithms of MSRCR, GFR, and the dark prior principle but slightly lower than the FMR algorithm due to the overall high grayscale value of FMR. The average gradient is higher than the MSRCR and Dark channel prior algorithms, and the improvement compared to MSRCR algorithm is 9.95%. The standard deviation of the image is 40.0% higher than the original image, which is better than other algorithms. The standard deviation is improved by 1.9% compared to the MSRCR algorithm. The average grayscale value of the image is low, indicating an overall low grayscale value, and the signal-to-noise ratio of the image is higher than the Dark channel prior and FMR algorithms but slightly lower than the MSRCR and GFR algorithms. Among them, the GFR algorithm has the highest signal-to-noise ratio and best fidelity.

CONCLUSIONS

In this study, a Retinex algorithm based on Tophat weighted bilateral filtering was proposed for images captured under extremely dense fog conditions. The foggy image is converted from RGB to HSV space, and the illumination component is enhanced. The modified Tophat operator is used as the filter function to convolve with the brightness component through the bilateral filter, which maintains the edge effect of the illumination component. Next, adaptive gamma correction is applied to correct the saturation component. Finally, the hue, reflection component, and corrected saturation component are merged through the reverse transformation of HSV-RGB to obtain the enhanced image. The experimental results show that the proposed algorithm has good enhancement effects for both close-range and distant view images captured under extremely heavy fog conditions. The proposed algorithm shows significant improvements in image sharpness, halo phenomena, anti-color distortion, and edge preservation. After enhancement, the image features have shown improvements in information entropy, standard deviation, mean gradient, and variance, indicating good enhancement effects for heavy foggy images.

ACKNOWLEDGMENT

This work was supported by the Anhui Educational Science Research Project 2024AH050520 and 2023AH051710. The School Projects zjqr23001 and zjqr23002 of Anhui Sanlian University.

REFERENCES

[1] Z. Li and S. Yang, Single image defogging based on variational Bayesian factor analysis, Signal Processing: Image Communication, vol. 105, 2022, pp. 116410.

[2] Y. Tsai, S. Lin, and L. Lien, Single image haze removal based on contrast enhancement and bilateral filter, IEEE Transactions on Circuits and Systems for Video Technology, vol. 30, no. 1, 2020, pp. 1-12.

[3] Liu F. An overview of image enhancement dehazing algorithms. Applied and Computational Engineering, 2023.

[4] Gnyawali D, Sigdel P R, Rai B D K, et al. Storz professional image enhancement system (SPECTRA A) enhancing detection of carcinoma urinary bladder by white light cystoscopy. African Journal of Urology, 2024, 30(1).

[5] Y. He, C. Guo, and J. Chen, Multi-scale retinex-based haze removal for outdoor images, International Journal of Remote Sensing, vol. 42, no. 11, 2021, pp. 3860-3879.

[6] Thilakanayake T, De Silva O, Wanasinghe T R, et al. A Generative Adversarial Network-based Method for LiDAR-Assisted Radar Image Enhancement. 2024.

[7] Zhang L, Yan L, Li S, et al. MMDCP: An Image Enhancement Algorithm Incorporating Multi-Channel Phase Activation and Multi-Constrained Dark Channel Prior. International Journal of Pattern Recognition and Artificial Intelligence, 2024, 38(04).

[8] Fabian K, Sven G, Desiree, Ehrmann-Müller, et al. Comparison of three different image enhancement systems for detection of laryngeal lesions. The Journal of laryngology and otology. 2024(1):138.
[9] X. Ji, J. Wang, G. Ma, and L. Cao, Single image dehazing via joint visual and scalar saliency guided pyramid decompositions, Signal Processing: Image Communication, vol. 80, 2020, pp. 115692.
[10] S. Wu, Y. Zhang, S. Gong, and Q. Cheng, Single image fog removal using bilateral filter and oriented diffusion, Signal Processing: Image Communication, vol. 94, 2021, pp. 116126.
[11] A. K. Tripathy, V. Singh, and K. K. Sarpatwar, Fog enhanced image retrieval using top-hat operator and Gaussian filters, Multimedia Tools and Applications, vol. 80, no. 13, 2021, pp. 19621-19644.
[12] Kumar R, Bhandari A K. Fundus image enhancement using visual transformation and maximum a posterior estimation. Biomedical Signal Processing and Control, 2023, 86: 105323.
[13] C. Zhu, Y. Lu, H. Jiang, and H. Zhang, Single-image defogging based on physical model and adaptive HSV color space conversion, Journal of Sensors, vol. 2021, pp. 5561718, 2021.
[14] Iqbal S, Khan T M, Naveed K, et al. Recent trends and advances in fundus image analysis: A review. Computers in Biology and Medicine, 2022: 106277.
[15] Popp A K, Schumacher M, Himstedt M. Adaptive Contrast Enhancement for Digital Radiographic Images using Image-to-Image Translation. Current Directions in Biomedical Engineering, 2024, 10(2):83-86.
[16] Rajpoot V, Mannepalli P K, Choubey S B, et al. A novel approach for weighted average filter and guided filter based on tunnel image enhancement. Journal of Intelligent & Fuzzy Systems, 2020, 39(3): 4597-4616.
[17] Jeba Derwin D, Jeba Singh O, Priestly Shan B, et al. An efficient multi-level pre-processing algorithm for the enhancement of dermoscopy images in Melanoma detection. Medical & Biological Engineering & Computing, 2023, 61(11): 2921-2938.
[18] Baig R, Bibi M, Hamid A, et al. Deep learning approaches towards skin lesion segmentation and classification from dermoscopic images-a review. Current Medical Imaging, 2020, 16(5): 513-533.
[19] Wen B. Application Research on Super-resolution of Downhole Image Based on Sparse Representation//2021 2nd International Conference on Computing, Networks and Internet of Things. 2021: 1-6.
[20] X. Zhang, X. Guan, and W. Zhu, Multi-level bilateral filter for fast and effective fog removal, IEEE Access, vol. 8, 2020, pp. 102306-102319.
[21] E. Corte-Real, A. Cunha, and J. Bernardino, Top-hat and bottom-hat transforms for unsupervised change detection in high resolution satellite images, IEEE Transactions on Geoscience and Remote Sensing, vol. 57, no. 11, 2019, pp. 9342-9357.
[22] B. Li, E. Chen, and R. Chen, A single image defogging algorithm based on improved multi-scale retinex and color correction, Proceedings of the 2020 5th International Conference on Machinery, Materials and Information Technology Applications, pp. 70-74, 2020.
[23] T. Guo, D. Zhao, and Y. Wu, An image defogging method based on guided filter and Retinex, Proceedings of the IEEE 3rd International Conference on Multimedia Information Processing and Retrieval, 2019, pp. 113-118.
[24] J. Tan, C. Xu, and Y. Chen, Single image defogging based on fusion of improved dark channel prior and guided filter, Journal of Electronic Imaging, vol. 30, no. 5, pp. 053013, 2021.
[25] Cooper T J, Baqai F A. Analysis and extensions of the Frankle-McCann Retinex algorithm. Journal of Electronic Imaging, 2019, 13(1):85-92.